JOURNAL OF MAGNETIC RESONANCE 33, 627–647 (1979)

NMR Shifts in Paramagnetic Systems: A Nonmultipole Expansion Method

R. M. GOLDING AND L. C. STUBBS

Department of Physical Chemistry, University of New South Wales, Box 1, P.O., Kensington, 2033, N.S.W., Australia

Received February 24, 1978; revised June 19, 1978

NMR shifts arising from the electron orbital angular momentum and the electron spin dipolar–nuclear spin angular momentum interactions using a nonmultipole expansion method are examined for a *d* electron in a crystal field of octahedral symmetry and with a tetragonal component. Bonding with the paramagnetic center is included. The NMR shifts are illustrated as isoshielding contour maps, and the results are compared with the multipole expansion method. It is shown that even when experimental data are successfully fitted by considering the NMR shifts as arising from the Fermi contact and the dipolar interactions, such an interpretation may lead to incorrect conclusions about the interactions within the paramagnetic system.

INTRODUCTION

Over the last few years the interpretation of the NMR shifts in d^n and f^n paramagnetic systems has been based upon the electron-nuclear interactions arising from the Fermi contact interaction, the electron orbital angular momentum, and the electron spin dipolar–nuclear spin angular momentum interactions. The latter two terms have been treated as a multipole expansion in R, where R is the distance between the NMR nucleus and the electron-bearing atom. In particular, the dipolar term in the expansion which is related to the magnetic susceptibility anisotropy (*1*) has been used almost exclusively, although more recently the higher multipole terms (2–5) have been evaluated for some specific examples. In a recent paper (*6*) we have shown that the use of such an expression may lead to serious errors in the interpretation of the NMR shift through this mechanism, especially if only the dipolar term is considered.

In some cases the Fermi contact interaction has been used to interpret the NMR shifts; see, for example, the NMR shifts in a series of transition metal ion dithiocarbamate complexes (*7*) and the ^{17}O NMR shifts of the aqueous trivalent lanthanide ions (*8*, *9*), where the NMR shift, ΔB, is given by

$$\Delta B = a\langle S_z\rangle / g_N\mu_N. \qquad [1]$$

Here a is the hyperfine interaction constant. In other cases the dipolar term in the multipole expansion has been used; see, for example, the proton NMR shifts in some

0022-2364/79/030627-21$02.00/0

lanthanide complexes (*10*), where in terms of the magnetic susceptibility components (*1*) $\chi_{\alpha\alpha}$

$$\Delta B/B = -(\mu_0/4\pi)[\{\chi_{zz} - \tfrac{1}{2}(\chi_{xx} + \chi_{yy})\}(3\cos^2\Theta - 1) + \tfrac{3}{2}(\chi_{xx} - \chi_{yy})\sin^2\Theta\cos 2\Phi]/3R^3. \quad [2]$$

The polar coordinates of the NMR nucleus in relation to the paramagnetic center are (R, Θ, Φ), where the z-axis is the principal axis of the complex. However, both the Fermi contact contribution given by [1] and the dipolar contribution given by [2] may be important (*11*). Recently (*12*) a method has been developed whereby, from a set of experimental results, an estimate may be made of the various contributions to the NMR shifts.

However, few publications have been devoted to the determination of the region where the dipolar contribution given by [2] may yield a good approximation. This is of special importance when there is delocalization of the unpaired electrons from the paramagnetic center. For example, it has been shown (*6*) that the ^{14}N NMR shift in the $Fe(CN)_6^{3-}$ ion may be interpreted as arising dominantly from the interaction with the nitrogen nucleus of the unpaired electrons in the nitrogen p orbital of the $^2T_2$ molecular orbitals.

In this paper we examine the NMR shifts arising from the electron orbital angular momentum and the electron spin dipolar–nuclear spin angular momentum interactions using the nonmultipole expansion method (*13*, *14*) (i.e., applicable for any **R**) for a number of specific cases. We include the effect of bonding with the paramagnetic center. The results are compared with the multipole expansion method. Finally, we show that even when the multipole expansion method gives errors, experimental shifts may still be fitted successfully using a combination of [1] and [2] but will lead to incorrect conclusions about the interactions within the paramagnetic system.

THEORY

The principal values σ_{xx}, σ_{yy}, and σ_{zz} of the NMR screening tensor $\boldsymbol{\sigma}$ are determined by considering the magnetic field interaction as parallel to the x, y, and z directions and averaged assuming a Boltzmann distribution.

The contribution to the NMR shift, ΔB, is given by

$$\Delta B = \tfrac{1}{3}B(\sigma_{xx} + \sigma_{yy} + \sigma_{zz}), \quad [3]$$

where

$$\sigma_{\alpha\alpha} = \left(\frac{\partial^2\langle\mathcal{H}\rangle}{\partial\mu_\alpha\,\partial B_\alpha}\right)_{\boldsymbol{\mu}=\mathbf{B}=\mathbf{0}},$$

where

$$\boldsymbol{\mu} = g_N\mu_N\mathbf{I}.$$

$\langle\mathcal{H}\rangle$ refers to the Boltzmann average of the hyperfine interaction represented by the Hamiltonian

$$\mathcal{H} = \frac{\mu_0}{4\pi}g_N\mu_B\mu_N\left\{\frac{2\mathbf{l}_N\cdot\mathbf{I}}{r_N^3} + g_s\left[\frac{3(\mathbf{r}_N\cdot\mathbf{s})\mathbf{r}_N\cdot\mathbf{I}}{r_N^5} - \frac{\mathbf{s}\cdot\mathbf{I}}{r_N^3}\right]\right\}. \quad [4]$$

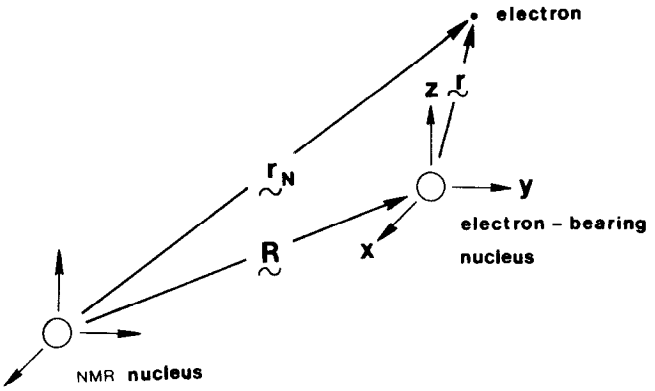

FIG. 1. The coordinate system.

In this paper we take g_s to be equal to 2 exactly. Here $\mathbf{r}_N$ is the radius vector of the electron about the nucleus with nuclear spin angular momentum **I**, as shown in Fig. 1.

The system we consider is a d^1 system in a strong crystal field of octahedral symmetry, where bonding effects have been incorporated using a molecular orbital approach. The paramagnetic site is surrounded by six ligands lying at a distance $\pm R_L$ along each of the three axes. It was assumed that the ligands could be treated as single atoms with three p orbitals available for bonding. The p orbitals parallel to the x, y, and z axes for the jth ligand are written as $|x_j\rangle$, $|y_j\rangle$, and $|z_j\rangle$, respectively. The numbering of the ligands is as shown in Fig. 2.

The appropriate molecular orbitals are (*15*)

$$\begin{aligned} &a|\xi\rangle+(b/2)[|y_5\rangle-|y_6\rangle+|z_2\rangle-|z_4\rangle], \\ &a|\eta\rangle+(b/2)[|z_1\rangle-|z_3\rangle+|x_5\rangle-|x_6\rangle], \\ &a|\zeta\rangle+(b/2)[|x_2\rangle-|x_4\rangle+|y_1\rangle-|y_3\rangle], \end{aligned} \qquad [5]$$

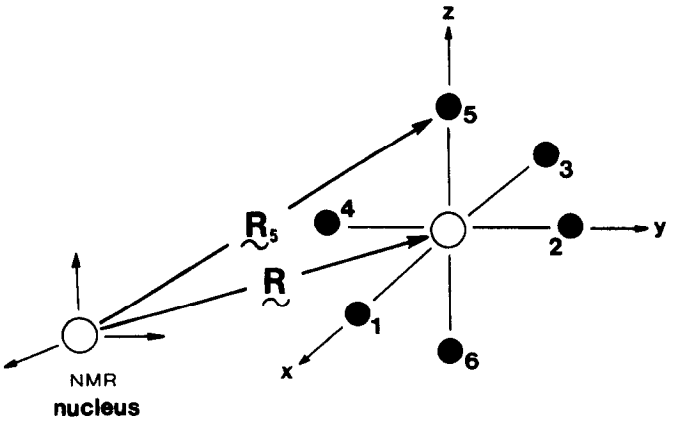

FIG. 2. The numbering of the ligands.

where the d orbitals are taken to be Slater-type 3d orbitals and are defined as

$$\begin{aligned} |\xi\rangle &= (2\beta_2^7/3\pi)^{1/2} yz \exp(-\beta_2 r), \\ |\eta\rangle &= (2\beta_2^7/3\pi)^{1/2} zx \exp(-\beta_2 r), \\ |\zeta\rangle &= (2\beta_2^7/3\pi)^{1/2} xy \exp(-\beta_2 r), \end{aligned} \tag{6}$$

and similarly the p orbitals are taken to be Slater-type $2p$ orbitals defined as

$$\begin{aligned} |x\rangle &= (\beta_1^5/\pi)^{1/2} x \exp(-\beta_1 r), \\ |y\rangle &= (\beta_1^5/\pi)^{1/2} y \exp(-\beta_1 r), \\ |z\rangle &= (\beta_1^5/\pi)^{1/2} z \exp(-\beta_1 r). \end{aligned} \tag{7}$$

The coefficients a and b in the molecular orbitals are defined from

$$\begin{aligned} k' &= a^2 + \tfrac{1}{2}b^2 + 3ab\langle d|p\rangle, \\ 1 &= a^2 + b^2 + 4ab\langle d|p\rangle, \end{aligned} \tag{8}$$

where k' is the orbital reduction factor and $\langle d|p\rangle$ gives the amount of overlap. The $^2T_2$ ground state of the d^1 system is split by spin–orbit coupling into two levels with respective eigenvalues of $-\frac{1}{2}\zeta'$ and ζ', where

$$\zeta' = (2k' - 1)\zeta_d + (1 - k')\zeta_p$$

where ζ_d and ζ_p are the spin–orbit coupling constants for the d and p orbitals, respectively.

The NMR shift is given by

$$\frac{\Delta B}{B} = \frac{2}{3}\frac{\mu_0}{4\pi}\frac{\mu_B^2}{kT}\left[\frac{E + F\exp(3\zeta'/2kT) + G\{1 - \exp(3\zeta'/2kT)\}kT/\zeta'}{1 + 2\exp(3\zeta'/2kT)}\right], \tag{9}$$

where

$$\begin{aligned} E &= \tfrac{1}{9}(2k' + 1)(D - 2L), \\ F &= \tfrac{1}{9}(1 - k')(D + 12L), \\ G &= \tfrac{2}{27}(k' + 2)(D + 4L), \end{aligned}$$

where

$$D = a^2 D_0(\mathbf{R}) + \frac{b^2}{4}\sum_{i=1}^{6} D_i(\mathbf{R}_i),$$

$$L = a^2 L_0(\mathbf{R}) + \frac{b^2}{4}\sum_{i=1}^{6} L_i(\mathbf{R}_i),$$

where $\mathbf{R}_i$ is the vector pointing from the NMR nucleus to the ith ligand. As an example, $\mathbf{R}_5$ is shown in Fig. 2. The functions $D_0(\mathbf{R})$ and $L_0(\mathbf{R})$ arising from the d

orbitals are

$$D_0(\mathbf{R}) = -\frac{32{,}400}{\beta_2^4 R^7}\left(\frac{\pi}{26}\right)^{1/2}\left[\frac{7}{4}^{1/2} Y_{64}(\Theta,\Phi) - \frac{1}{2(2)^{1/2}} Y_{60}(\Theta,\Phi) + \frac{7^{1/2}}{4} Y_{6-4}(\Theta,\Phi)\right] S(t_0)$$
$$-\frac{672}{\beta_2^2 R^5}\left(\frac{\pi}{21}\right)^{1/2}\left[\frac{1}{2}\left(\frac{5}{6}\right)^{1/2} Y_{44}(\Theta,\Phi) + \frac{1}{2}\left(\frac{7}{3}\right)^{1/2} Y_{40}(\Theta,\Phi) + \frac{1}{2}\left(\frac{5}{6}\right)^{1/2} Y_{4-4}(\Theta,\Phi)\right] F(t_0)$$
$$+\frac{4\beta_2^3}{35}\pi^{1/2}[Y_{00}(\Theta,\Phi)] N(t_0) \qquad [10a]$$

and

$$L_0(\mathbf{R}) = \frac{168}{\beta_2^2 R^5}\left(\frac{\pi}{21}\right)^{1/2}\left[\frac{1}{2}\left(\frac{5}{6}\right)^{1/2} Y_{44}(\Theta,\Phi) + \frac{1}{2}\left(\frac{7}{3}\right)^{1/2} Y_{40}(\Theta,\Phi) + \frac{1}{2}\left(\frac{5}{6}\right)^{1/2} Y_{4-4}(\Theta,\Phi)\right] K(t_0) + \frac{2\beta_2^3}{5}\pi^{1/2}[Y_{00}(\Theta,\Phi)] M(t_0), \qquad [10b]$$

where $t_0 = 2\beta_2 R$ and

$$S(t) = \left[1 - e^{-t}\sum_{n=0}^{11}\frac{t^n}{n!}\right],$$
$$F(t) = \left[1 - e^{-t}\left(\frac{12}{11}\frac{t^9}{9!} + \sum_{n=0}^{8}\frac{t^n}{n!}\right)\right],$$
$$N(t) = \left[e^{-t}\left(-\frac{t^4}{18} + \frac{t^3}{3!} + \frac{t^2}{2!} + t + 1\right)\right],$$
$$K(t) = \left[1 - e^{-t}\sum_{n=0}^{8}\frac{t^n}{n!}\right],$$
$$M(t) = \left[e^{-t}\left(\frac{t^3}{3!} + \frac{t^2}{2!} + t + 1\right)\right].$$

The functions $D_i(\mathbf{R}_i)$ and $L_i(\mathbf{R}_i)$ $(i = 1, \ldots, 6)$ arising from the p orbitals on the ith ligand are given by

$$D_1(\mathbf{R}_1) = -\frac{72\pi^{1/2}}{\beta_1^2 R_1^5}\left[\frac{1}{3}\left(\frac{5}{2}\right)^{1/2} Y_{42}(\Theta_1,\Phi_1) + \frac{2}{3} Y_{40}(\Theta_1,\Phi_1) + \frac{1}{3}\left(\frac{5}{2}\right)^{1/2} Y_{4-2}(\Theta_1,\Phi_1)\right] H(t_1)$$
$$-\frac{4}{R_1^3}\left(\frac{\pi}{5}\right)^{1/2}\left[\frac{1}{2}\left(\frac{3}{2}\right)^{1/2} Y_{22}(\Theta_1,\Phi_1) - \frac{1}{2} Y_{20}(\Theta_1,\Phi_1) + \frac{1}{2}\left(\frac{3}{2}\right)^{1/2} Y_{2-2}(\Theta_1,\Phi_1)\right] I(t_1) + \frac{4\beta_1^3}{15}\pi^{1/2}[Y_{00}(\Theta_1,\Phi_1)] J(t_1), \qquad [11a]$$

$$L_1(\mathbf{R}_1) = \frac{2}{R_1^3}\left(\frac{\pi}{5}\right)^{1/2}\left[\frac{1}{2}\left(\frac{3}{2}\right)^{1/2} Y_{22}(\Theta_1, \Phi_1) - \frac{1}{2} Y_{20}(\Theta_1, \Phi_1)\right.$$
$$\left. + \frac{1}{2}\left(\frac{3}{2}\right)^{1/2} Y_{2-2}(\Theta_1, \Phi_1)\right] T(t_1)$$
$$+ \frac{2\beta_1^3}{3}\pi^{1/2}[Y_{00}(\Theta_1, \Phi_1)]C(t_1), \qquad [11b]$$

$$D_2(\mathbf{R}_2) = \frac{72\pi^{1/2}}{\beta_1^2 R_2^5}\left[\frac{1}{3}\left(\frac{5}{2}\right)^{1/2} Y_{42}(\Theta_2, \Phi_2) - \frac{2}{3} Y_{40}(\Theta_2, \Phi_2)\right.$$
$$\left. + \frac{1}{3}\left(\frac{5}{2}\right)^{1/2} Y_{4-2}(\Theta_2, \Phi_2)\right] H(t_2)$$
$$+ \frac{4}{R_2^3}\left(\frac{\pi}{5}\right)^{1/2}\left[\frac{1}{2}\left(\frac{3}{2}\right)^{1/2} Y_{22}(\Theta_2, \Phi_2) + \frac{1}{2} Y_{20}(\Theta_2, \Phi_2)\right.$$
$$\left. + \frac{1}{2}\left(\frac{3}{2}\right)^{1/2} Y_{2-2}(\Theta_2, \Phi_2)\right] I(t_2) + \frac{4\beta_1^3}{15}\pi^{1/2}[Y_{00}(\Theta_2, \Phi_2)]J(t_2), \qquad [11c]$$

$$L_2(\mathbf{R}_2) = -\frac{2}{R_2^3}\left(\frac{\pi}{5}\right)^{1/2}\left[\frac{1}{2}\left(\frac{3}{2}\right)^{1/2} Y_{22}(\Theta_2, \Phi_2) + \frac{1}{2} Y_{20}(\Theta_2, \Phi_2)\right.$$
$$\left. + \frac{1}{2}\left(\frac{3}{2}\right)^{1/2} Y_{2-2}(\Theta_2, \Phi_2)\right] T(t_2) + \frac{2\beta_1^3}{3}\pi^{1/2}[Y_{00}(\Theta_2, \Phi_2)]C(t_2), \qquad [11d]$$

$$D_5(\mathbf{R}_5) = -\frac{72\pi^{1/2}}{\beta_1^2 R_5^5}\left[\frac{1}{6}\left(\frac{35}{2}\right)^{1/2} Y_{44}(\Theta_5, \Phi_5) - \frac{1}{6} Y_{40}(\Theta_5, \Phi_5)\right.$$
$$\left. + \frac{1}{6}\left(\frac{35}{2}\right)^{1/2} Y_{4-4}(\Theta_5, \Phi_5)\right] H(t_5)$$
$$- \frac{4}{R_5^3}\left(\frac{\pi}{5}\right)^{1/2}[Y_{20}(\Theta_5, \Phi_5)]I(t_5) + \frac{4\beta_1^3}{15}\pi^{1/2}[Y_{00}(\Theta_5, \Phi_5)]J(t_5), \qquad [11e]$$

$$L_5(\mathbf{R}_5) = \frac{2}{R_5^3}\left(\frac{\pi}{5}\right)^{1/2}[Y_{20}(\Theta_5, \Phi_5)]T(t_5) + \frac{2\beta_1^3}{3}\pi^{1/2}[Y_{00}(\Theta_5, \Phi_5)]C(t_5), \qquad [11f]$$

and

$$D_3(\mathbf{R}_3) = D_1(\mathbf{R}_3); \qquad L_3(\mathbf{R}_3) = L_1(\mathbf{R}_3),$$

$$D_4(\mathbf{R}_4) = D_2(\mathbf{R}_4); \qquad L_4(\mathbf{R}_4) = L_2(\mathbf{R}_4),$$

$$D_6(\mathbf{R}_6) = D_5(\mathbf{R}_6); \qquad L_6(\mathbf{R}_6) = L_5(\mathbf{R}_6),$$

where $t_i = 2\beta_1 R_i$ and

$$H(t) = \left[1 - e^{-t} \sum_{n=0}^{7} \frac{t^n}{n!}\right],$$

$$I(t) = \left[1 - e^{-t}\left(\frac{5}{504} t^5 + \sum_{n=0}^{4} \frac{t^n}{n!}\right)\right],$$

$$J(t) = \left[e^{-t}\left(-\frac{t^2}{3} + t + 1\right)\right],$$

$$T(t) = \left[1 - e^{-t} \sum_{n=0}^{4} \frac{t^n}{n!}\right],$$

$$C(t) = [e^{-t}(t+1)].$$

When bonding effects are neglected (that is, taking $a^2 = 1$ and $b^2 = 0$), the results reduce to those given by Golding and Stubbs (*14*).

In arriving at this expression for the NMR shift many molecular hyperfine integrals had to be evaluated. The full set of integrals for the $2p$ orbitals is given in the Appendix.

The results given by Golding and Stubbs (*14, 16*) for the components of the hyperfine interaction tensors for the $^2T_2E''$ and $^2T_2U'$ levels may be extended to incorporate bonding effects by replacing, in the appropriate formulas for the tensor components,

$$\langle\xi|T_{\alpha\beta}|\xi\rangle, \quad \langle\eta|T_{\alpha\beta}|\eta\rangle, \quad \langle\zeta|T_{\alpha\beta}|\zeta\rangle,$$
$$\langle\xi|T_{\alpha\beta}|\eta\rangle, \quad \langle\eta|T_{\alpha\beta}|\zeta\rangle, \quad \langle\zeta|T_{\alpha\beta}|\xi\rangle,$$
$$\langle\eta|l_{N\alpha}/r_N^3|\xi\rangle, \quad \langle\zeta|l_{N\alpha}/r_N^3|\eta\rangle, \quad \langle\xi|l_{N\alpha}/r_N^3|\zeta\rangle,$$

where

$$T_{\alpha\beta} = (3r_{N\alpha}r_{N\beta} - r_N^2\delta_{\alpha\beta})/r_N^5,$$

by

$$a^2\langle\xi|T_{\alpha\beta}|\xi\rangle + (b^2/4)[\langle z_2|T_{\alpha\beta}|z_2\rangle + \langle z_4|T_{\alpha\beta}|z_4\rangle + \langle y_5|T_{\alpha\beta}|y_5\rangle + \langle y_6|T_{\alpha\beta}|y_6\rangle],$$
$$a^2\langle\eta|T_{\alpha\beta}|\eta\rangle + (b^2/4)[\langle x_5|T_{\alpha\beta}|x_5\rangle + \langle x_6|T_{\alpha\beta}|x_6\rangle + \langle z_1|T_{\alpha\beta}|z_1\rangle + \langle z_3|T_{\alpha\beta}|z_3\rangle],$$
$$a^2\langle\zeta|T_{\alpha\beta}|\zeta\rangle + (b^2/4)[\langle y_1|T_{\alpha\beta}|y_1\rangle + \langle y_3|T_{\alpha\beta}|y_3\rangle + \langle x_2|T_{\alpha\beta}|x_2\rangle + \langle x_4|T_{\alpha\beta}|x_4\rangle],$$
$$a^2\langle\xi|T_{\alpha\beta}|\eta\rangle + (b^2/4)[\langle y_5|T_{\alpha\beta}|x_5\rangle + \langle y_6|T_{\alpha\beta}|x_6\rangle],$$
$$a^2\langle\eta|T_{\alpha\beta}|\zeta\rangle + (b^2/4)[\langle z_1|T_{\alpha\beta}|y_1\rangle + \langle z_3|T_{\alpha\beta}|y_3\rangle],$$
$$a^2\langle\zeta|T_{\alpha\beta}|\xi\rangle + (b^2/4)[\langle x_2|T_{\alpha\beta}|z_2\rangle + \langle x_4|T_{\alpha\beta}|z_4\rangle],$$
$$a^2\langle\eta|l_{N\alpha}/r_N^3|\xi\rangle + (b^2/4)[\langle x_5|l_{N\alpha}/r_N^3|y_5\rangle + \langle x_6|l_{N\alpha}/r_N^3|y_6\rangle],$$
$$a^2\langle\zeta|l_{N\alpha}/r_N^3|\eta\rangle + (b^2/4)[\langle y_1|l_{N\alpha}/r_N^3|z_1\rangle + \langle y_3|l_{N\alpha}/r_N^3|z_3\rangle],$$

and

$$a^2\langle\xi|l_{N\alpha}/r_N^3|\zeta\rangle + (b^2/4)[\langle z_2|l_{N\alpha}/r_N^3|x_2\rangle + \langle z_4|l_{N\alpha}/r_N^3|x_4\rangle],$$

respectively.

DISCUSSION

Initially we examine the case for a d^1 transition metal ion in a strong crystal field of octahedral symmetry where the transition metal ion is surrounded by six ligands all 0.2 nm from the central atom along the three axes. We choose $\beta_1 = 2.275/a_0$ and $\beta_2 = 2.2/a_0$, the temperature as $T = 300$ K, the bonding coefficients as $a = 0.8154$ and $b = -0.6818$, and the spin–orbit coupling constants as $\zeta_d = 400\ \text{cm}^{-1}$ and $\zeta_p = 110\ \text{cm}^{-1}$. The overlap integral $\langle d|p\rangle = 0.0584$. The contours of equal chemical shift $\Delta B/B$ in parts per million in the xy plane as determined from the expression given in the previous section are shown in Fig. 3. The contour map is very complex and is markedly different for the case when no bonding is considered; see Fig. 4. In

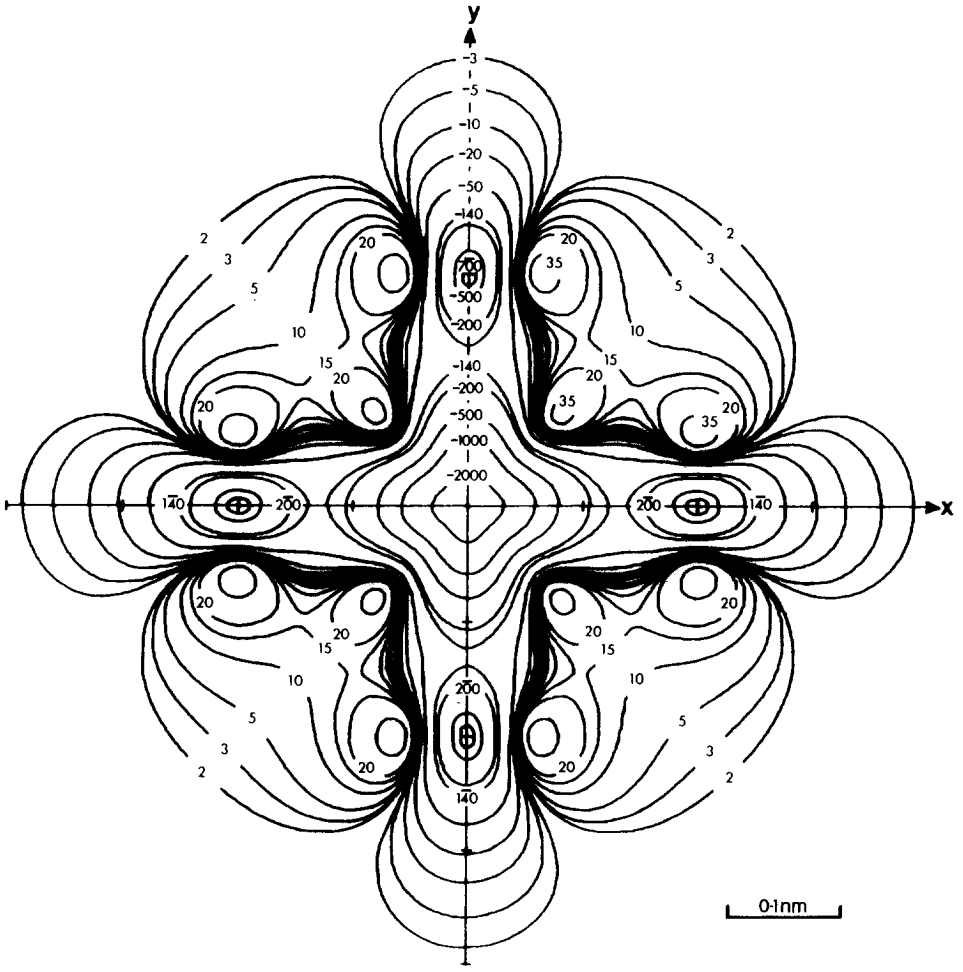

FIG. 3. An isoshielding diagram for the case of the NMR nucleus in the xy plane for a d^1 transition metal ion in a strong crystal field of octahedral symmetry, where bonding effects have been considered. Ligands are located at ±0.2 nm from the central metal ion along the three axes. The contours of equal chemical shift $\Delta B/B$ are in parts per million. (A bar over a number indicates a negative value.)

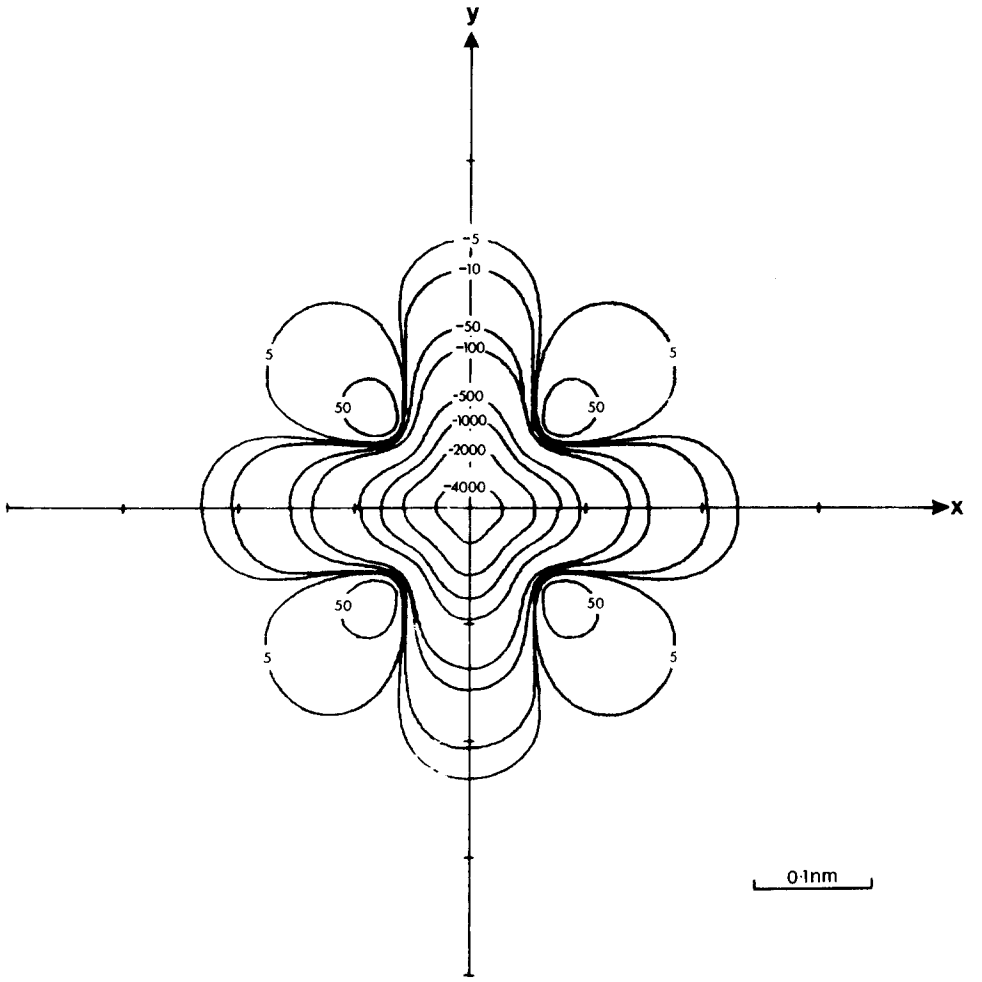

FIG. 4. An isoshielding diagram for the case of the NMR nucleus in the xy plane for a d^1 transition metal ion in a strong crystal field of octahedral symmetry, for the case when bonding is not considered. The contours of equal chemical shift $\Delta B/B$ are in parts per million.

Fig. 3 near the transition metal ion and the six ligands, $\Delta B/B$ is nearly isotropic. There are a number of regions where $\Delta B/B$ is a maximum or a minimum and regions where $\Delta B/B$ changes rapidly with distance. The pattern in Fig. 3 gives an insight into the very complex manner in which the NMR shift varies throughout the molecular system.

Next we examine the reliability of considering the NMR shift in specific regions in space for the system given by Fig. 2 using the multipole expansion approach. A comparison of the exact solution with all the multipolar terms and only the dipolar term is given in Table 1 at different values of R along the ⟨100⟩, ⟨110⟩, and ⟨111⟩ axes. In this particular case the dipolar term arises only from the ligand part of the electronic wavefunction. From Table 1 we observe that consideration of the dipolar

TABLE 1

A COMPARISON, FOR DIFFERENT VALUES OF R ALONG ⟨100⟩, ⟨110⟩, AND ⟨111⟩ AXES, OF THE RESULTS FOR $\Delta B/B$ USING (a) THE EXACT SOLUTION; (b) THE MULTIPOLAR EXPANSION; AND (c) THE POINT-DIPOLE APPROXIMATION

	$\Delta B/B$ along a ⟨100⟩ axis (ppm)			$\Delta B/B$ along a ⟨110⟩ axis (ppm)			$\Delta B/B$ along a ⟨111⟩ axis (ppm)		
R (nm)	(a) Exact	(b) Multipolar	(c) Dipolar	(a) Exact	(b) Multipolar	(c) Dipolar	(a) Exact	(b) Multipolar	(c) Dipolar
0.05	−1294.244	−57,714.116	−13.543	−803.132	89,840.682	−12.953	−935.934	−95,644.784	−12.803
0.1	−244.203	−545.230	−22.454	28.633	708.003	−10.759	−134.595	−712.930	−9.734
0.15	−177.257	−350.816	−141.984	23.388	43.189	−3.842	−25.103	−41.367	−3.492
0.2	−820.166	—	—	11.232	12.076	1.802	−4.703	−5.289	0.743
0.25	−145.109	−313.601	−139.897	6.090	6.145	2.477	−0.429	−0.451	1.691
0.3	−22.274	−23.381	−17.523	2.955	2.958	1.589	0.439	0.438	1.364
0.35	−6.011	−6.023	−5.133	1.408	1.408	0.874	0.495	0.495	0.904
0.4	−2.350	−2.350	−2.105	0.699	0.699	0.475	0.384	0.384	0.571
0.45	−1.124	−1.124	−1.032	0.367	0.367	0.266	0.272	0.272	0.361
0.5	−0.606	−0.606	−0.566	0.205	0.205	0.155	0.188	0.188	0.233
0.55	−0.355	−0.355	−0.335	0.120	0.120	0.095	0.130	0.130	0.153
0.6	−0.221	−0.221	−0.210	0.074	0.074	0.060	0.091	0.091	0.104
0.65	−0.144	−0.144	−0.138	0.047	0.047	0.039	0.064	0.064	0.072
0.7	−0.097	−0.097	−0.094	0.032	0.032	0.027	0.046	0.046	0.051

term only gives rise to substantial errors at distances less than 0.7 nm from the paramagnetic center. However, by considering all the multipolar terms the agreement with the exact solution occurs at distances greater than 0.4 nm.

In many cases experimental paramagnetic NMR shifts are analyzed in terms of the Fermi contact and the dipolar interactions given by Eqs. [1] and [2]. To explore the possible problems of interpretation associated by such a procedure we examine the $\Delta B/B$ results obtained from the previous section over a temperature range and reconsider the data as a set of experimental results. We attempt to analyze the data when a ligand atom is the NMR nucleus as arising from a sum of the Fermi contact and the dipolar interactions given by Eqs. [1] and [2]. In this paper we choose $\langle S_z \rangle$ in Eq. [1] as given in Ref. (*17*) for a d^1 ion in a crystal field of octahedral symmetry. In the evaluation of $\chi_\parallel$ and $\chi_\perp$ we include a small tetragonal distortion from octahedral symmetry. The quantities $\chi_\parallel$ and $\chi_\perp$ are determined from expressions in Ref. (*15*), where δ is a measure of the distortion from octahedral symmetry. The δ value is adjusted to give the best fit of the theoretical values of ΔB to the expression

$$\Delta B = a\langle S_z \rangle + b(\chi_\parallel - \chi_\perp).$$

In this case the best fit is obtained over the temperature range 200 to 400 K by choosing a very small distortion, and the results are summarized in Table 2. From Table 2 it follows that the analysis of the data using Eqs. [1] and [2] would incorrectly imply that the NMR shift arises dominantly from the Fermi contact interaction with a small contribution from the dipolar term in the multipole expansion. Although the case above was chosen when the ligand was the NMR nucleus, similar analyses may be made when the NMR nucleus is at any other position within the molecular system.

TABLE 2

A SUMMARY OF THE RESULTS OF FITTING A SET OF THEORETICAL DATA FOR $\Delta B/B$ AS ARISING FROM A SUM OF THE FERMI CONTACT AND DIPOLAR INTERACTIONS AS GIVEN BY EQS. [1] AND [2], FOR THE CASE OF A d^1 TRANSITION METAL ION IN A STRONG CRYSTAL FIELD OF OCTAHEDRAL SYMMETRY, WHERE BONDING EFFECTS HAVE BEEN CONSIDERED

		$\Delta B/B$ fitted to Eqs. [1] and [2]		
T (K)	$\Delta B/B$ (ppm) Exact	Contribution from [1]	Contribution from [2]	Total
200	−644.4	−938.8	293.0	−645.8
220	−706.8	−932.1	225.9	−706.2
240	−752.1	−923.9	173.2	−750.7
260	−784.2	−914.3	131.6	−782.7
280	−806.2	−903.5	98.6	−804.9
300	−820.2	−891.6	72.2	−819.4
320	−828.0	−878.9	51.0	−827.9
340	−831.0	−865.5	34.1	−831.4
360	−830.3	−851.7	20.4	−831.3
380	−826.8	−837.5	9.5	−828.0
400	−820.9	−823.2	0.7	−822.5

Hence, we have demonstrated that it does not necessarily follow that a good fit of a combination of Eqs. [1] and [2] to a set of experimental data results in a correct understanding of the origin of the NMR shift.

Finally, employing results given in (*14*), we examine the $\Delta B/B$ contour map for a d^1 octahedral metal ion system where the crystal field environment is of tetragonal symmetry with the tetragonal distortion along the z axis. We neglect bonding in this example. The tetragonal distortion component of the crystal field interaction was chosen in the form $\delta(l_z^2 - 2)$, where δ, the distortion parameter, was taken as 1000 cm^{-1}. With $\zeta_d = 400\ cm^{-1}$, $\beta_2 = 2.2/a_0$, and $T = 300$ K, the position of the NMR nucleus relative to the d-electron-bearing atom to give rise to a specific NMR

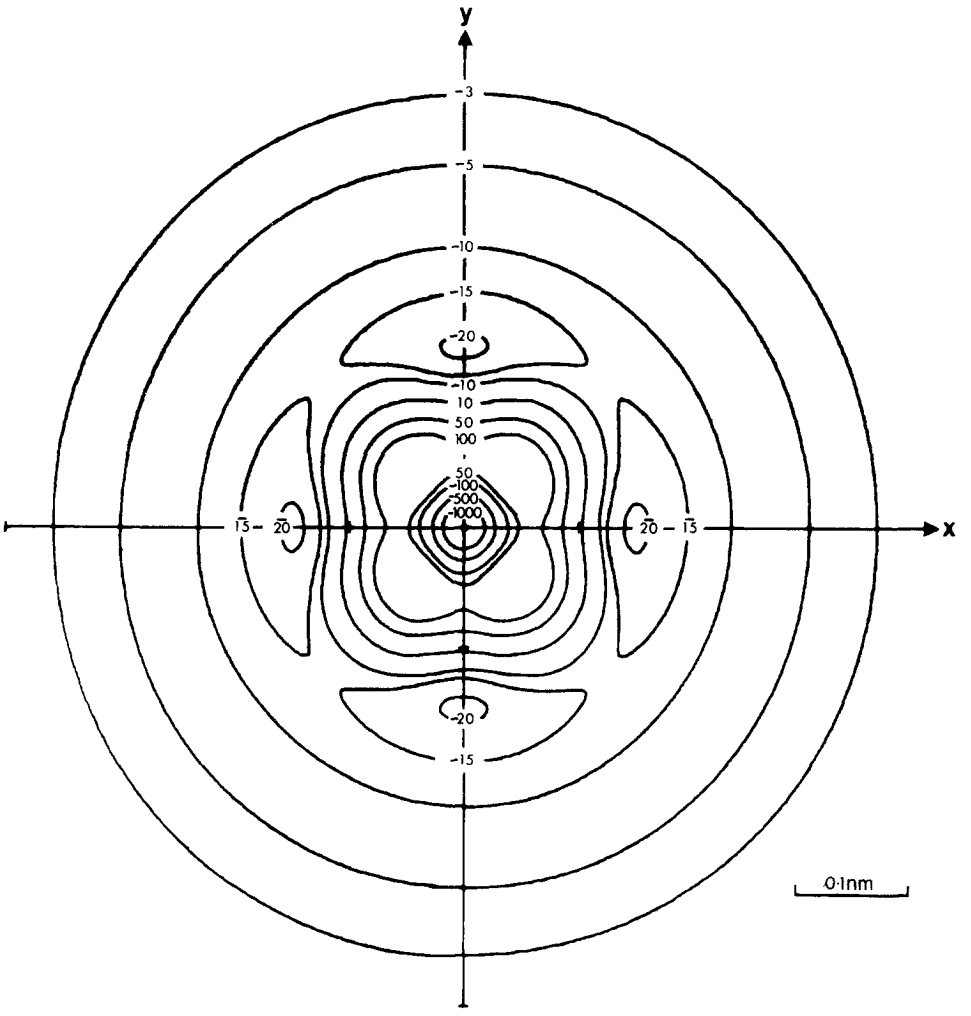

FIG. 5. An isoshielding diagram for the case of the NMR nucleus in the xy plane for a d^1 transition metal ion in a strong crystal field of tetragonal symmetry for $\delta = 1000\ cm^{-1}$, $\zeta_d = 400\ cm^{-1}$, $\beta_2 = 2.2/a_0$, and $T = 300$ K. The contours of equal chemical shift $\Delta B/B$ are in parts per million. (A bar over a number indicates a negative value.)

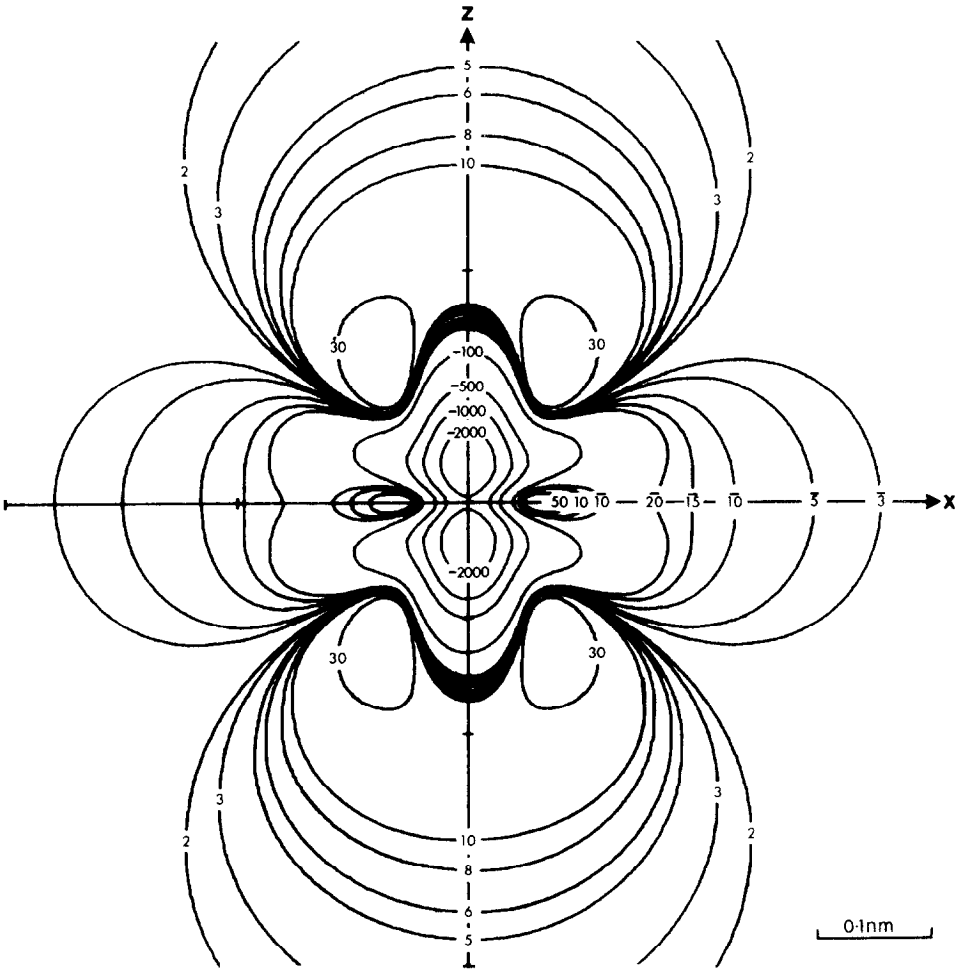

FIG. 6. An isoshielding diagram for the case of the NMR nucleus in the zx plane for a d^1 transition metal ion in a strong crystal field of tetragonal symmetry for $\delta = 1000\ \text{cm}^{-1}$, $\zeta_d = 400\ \text{cm}^{-1}$, $\beta_2 = 2.2/a_0$, and $T = 300$ K. The contours of equal chemical shift $\Delta B/B$ are in parts per million. (A bar over a number indicates a negative value.)

shift, $\Delta B/B$, was determined as a set of isoshielding contours. The $\Delta B/B$ contours in the xy and zx planes are shown in Figs. 5 and 6, respectively.

In the xy plane (see Fig. 5), the isoshielding lines form a complex pattern for R values less than 0.2 nm, whereas at larger values of R the contours, as expected, are independent of Φ. Similarly, in the zx plane (see Fig. 6), the isoshielding lines form a complex pattern for R values less than 0.3 nm. At very large values of R the pattern approaches the contours proportional to $(3\cos^2\Theta - 1)/R^3$. These diagrams illustrate clearly the complex patterns formed by the isoshielding lines for a wide range of R, namely, $R = 0$ to 0.5 nm.

To investigate further the method of using [1] and/or [2] to interpret paramagnetic NMR shifts, we choose a set of $\Delta B/B$ values over a temperature range for this case

TABLE 3

A SUMMARY OF THE RESULTS OF FITTING A SET OF THEORETICAL DATA FOR $\Delta B/B$ AS ARISING FROM A SUM OF THE FERMI CONTACT AND DIPOLAR INTERACTIONS AS GIVEN BY EQS. [1] AND [2], FOR THE CASE OF A d^1 TRANSITION METAL ION IN A STRONG CRYSTAL FIELD OF TETRAGONAL SYMMETRY

		$\Delta B/B$ fitted to Eqs. [1] and [2]		
T (K)	$\Delta B/B$ (ppm) Exact	Contribution from [1]	Contribution from [2]	Total
200	−35.56	−2.69	−32.91	−35.60
220	−30.19	−2.67	−27.51	−30.18
240	−25.37	−2.65	−22.71	−25.35
260	−21.12	−2.62	−18.49	−21.11
280	−17.41	−2.59	−14.82	−17.41
300	−14.19	−2.55	−11.65	−14.20
320	−11.41	−2.52	−8.92	−11.43
340	−9.03	−2.48	−6.57	−9.05
360	−6.98	−2.44	−4.55	−6.99
380	−5.24	−2.40	−2.83	−5.23
400	−3.74	−2.36	−1.35	−3.71

when the NMR nucleus is 0.2 nm along the x axis. The analysis of fitting the temperature dependence of $\Delta B/B$ for the exact solution for a tetragonal distortion component given by $\delta = 1000\ \text{cm}^{-1}$ to a combination of [1] and [2] is summarized in Table 3. Such an analysis yields a distortion parameter and a distance R from [2] of $650\ \text{cm}^{-1}$ and 0.220 nm, respectively, with substantial contributions from both the Fermi contact and dipolar interactions. The result further supports our previous finding that care needs to be exercised in interpreting NMR results of paramagnetic systems.

APPENDIX: MOLECULAR HYPERFINE INTEGRALS FOR $2p$ ORBITALS

(a) The Radial Series

The method of evaluating the molecular hyperfine integrals is that given by Golding and Stubbs (*14*). Define the radial integral

$$R_n^{(L)}(t) = 4\beta_1^5(-R)^L \int_0^\infty r_N^{1-L} b_n(R, r_N)\, dr_N$$

and

$$U_n(t) = R_n^{(2)}(t),$$
$$V_n(t) = R_n^{(1)}(t),$$
$$W_n(t) = R_n^{(0)}(t),$$

where $t = 2\beta_1 R$ and

$$b_n(R, r_N) = (r_>/r_<)^{1/2} I_{n+1/2}(2\beta_1 r_<) K_{n+3/2}(2\beta_1 r_>) - (r_</r_>)^{1/2} I_{n-1/2}(2\beta_1 r_<) K_{n+1/2}(2\beta_1 r_>),$$

where $r_<$ is the smaller of R and r_N and $r_>$ is the larger of R and r_N and I_ν and K_ν are the modified Bessel functions.

The following radial integrals for $2p$ orbitals are required:

$$U_2(t) = \beta_1^3\left[\frac{2}{t} - \left(\frac{t^2}{3} + t + 2 + \frac{2}{t}\right) e^{-t}\right],$$

$$V_1(t) = -\beta_1^3\left[\frac{2}{t} - \left(t + 2 + \frac{2}{t}\right) e^{-t}\right],$$

$$V_3(t) = -\beta_1^3\left[\left(\frac{2}{t} - \frac{40}{t^3}\right) + \left(\frac{2}{3}t + \frac{14}{3} + \frac{18}{t} + \frac{40}{t^2} + \frac{40}{t^3}\right) e^{-t}\right],$$

$$W_0(t) = \beta_1^3\left[\frac{2}{t} - \left(1 + \frac{2}{t}\right) e^{-t}\right],$$

$$W_2(t) = \beta_1^3\left[\left(\frac{2}{t} - \frac{24}{t^3}\right) + \left(2 + \frac{10}{t} + \frac{24}{t^2} + \frac{24}{t^3}\right) e^{-t}\right],$$

$$W_4(t) = \beta_1^3\left[\left(\frac{2}{t} - \frac{80}{t^3} + \frac{1680}{t^5}\right) - \left(\frac{8}{3} + \frac{32}{t} + \frac{200}{t^2} + \frac{760}{t^3} + \frac{1680}{t^4} + \frac{1680}{t^5}\right) e^{-t}\right].$$

(b) The Integrals $\langle \Psi_i | T_{\alpha\beta} | \Psi_j \rangle$

Employing the notation of Griffith (*18*), define

$$Z_{L0}(\Theta, \Phi) = Y_{L0}(\Theta, \Phi),$$
$$Z^{(c)}_{LM}(\Theta, \Phi) = (1/2^{1/2})[Y_{L-M}(\Theta, \Phi) + Y^*_{L-M}(\Theta, \Phi)],$$
$$Z^{(s)}_{LM}(\Theta, \Phi) = (i/2^{1/2})[Y_{L-M}(\Theta, \Phi) - Y^*_{L-M}(\Theta, \Phi)].$$

For the radial parts of the integrals define

$$f_n(a) = U_2 + aV_1 + (2-a)V_3 + W_n$$

The integrals $\langle \Psi_i | T_{\alpha\beta} | \Psi_j \rangle$ are

$$\langle x | T_{xx} | x \rangle = 2\left(\frac{\pi}{35}\right)^{1/2} f_4(0) Z^{(c)}_{44}(\Theta, \Phi) - \frac{4}{7}\left(\frac{\pi}{5}\right)^{1/2} f_4(0) Z^{(c)}_{42}(\Theta, \Phi) + \frac{6\pi^{1/2}}{35} f_4(0) Z_{40}(\Theta, \Phi) + \frac{22}{7}\left(\frac{\pi}{15}\right)^{1/2} f_2\left(\frac{56}{55}\right) Z^{(c)}_{22}(\Theta, \Phi) - \frac{22}{21}\left(\frac{\pi}{5}\right)^{1/2} f_2\left(\frac{56}{55}\right) Z_{20}(\Theta, \Phi) + \frac{8\pi^{1/2}}{15} f_0(2) Z_{00}(\Theta, \Phi),$$

$$\langle x|T_{yy}|x\rangle = -2\left(\frac{\pi}{35}\right)^{1/2} f_4(0)Z_{44}^{(c)}(\Theta,\Phi) + \frac{2\pi^{1/2}}{35} f_4(0)Z_{40}(\Theta,\Phi) - 2\left(\frac{\pi}{15}\right)^{1/2}$$
$$\times f_2\left(\frac{4}{5}\right)Z_{22}^{(c)}(\Theta,\Phi)$$
$$+\frac{2}{21}\left(\frac{\pi}{5}\right)^{1/2} f_2\left(\frac{28}{5}\right)Z_{20}(\Theta,\Phi) - \frac{4\pi^{1/2}}{15} f_0(2)Z_{00}(\Theta,\Phi),$$

$$\langle x|T_{zz}|x\rangle = \frac{4}{7}\left(\frac{\pi}{5}\right)^{1/2} f_4(0)Z_{42}^{(c)}(\Theta,\Phi) - \frac{8\pi^{1/2}}{35} f_4(0)Z_{40}(\Theta,\Phi) - \frac{8}{7}\left(\frac{\pi}{15}\right)^{1/2}$$
$$\times f_2\left(\frac{7}{5}\right)Z_{22}^{(c)}(\Theta,\Phi)$$
$$+\frac{20}{21}\left(\frac{\pi}{5}\right)^{1/2} f_2\left(\frac{14}{25}\right)Z_{20}(\Theta,\Phi) - \frac{4\pi^{1/2}}{15} f_0(2)Z_{00}(\Theta,\Phi),$$

$$\langle x|T_{xy}|x\rangle = 2\left(\frac{\pi}{35}\right)^{1/2} f_4(0)Z_{44}^{(s)}(\Theta,\Phi) - \frac{2}{7}\left(\frac{\pi}{5}\right)^{1/2} f_4(0)Z_{42}^{(s)}(\Theta,\Phi) + \frac{18}{7}\left(\frac{\pi}{15}\right)^{1/2}$$
$$\times f_2\left(\frac{14}{15}\right)Z_{22}^{(s)}(\Theta,\Phi),$$

$$\langle x|T_{yz}|x\rangle = \left(\frac{2\pi}{35}\right)^{1/2} f_4(0)Z_{43}^{(s)}(\Theta,\Phi) - \frac{1}{7}\left(\frac{2\pi}{5}\right)^{1/2} f_4(0)Z_{41}^{(s)}(\Theta,\Phi) + \frac{6}{7}\left(\frac{\pi}{15}\right)^{1/2}$$
$$\times f_2(0)Z_{21}^{(s)}(\Theta,\Phi),$$

$$\langle x|T_{zx}|x\rangle = \left(\frac{2\pi}{35}\right)^{1/2} f_4(0)Z_{43}^{(c)}(\Theta,\Phi) - \frac{3}{7}\left(\frac{2\pi}{5}\right)^{1/2} f_4(0)Z_{41}^{(c)}(\Theta,\Phi) + \frac{18}{7}\left(\frac{\pi}{15}\right)^{1/2}$$
$$\times f_2\left(\frac{14}{15}\right)Z_{21}^{(c)}(\Theta,\Phi),$$

$$\langle y|T_{xx}|y\rangle = -2\left(\frac{\pi}{35}\right)^{1/2} f_4(0)Z_{44}^{(c)}(\Theta,\Phi) + \frac{2\pi^{1/2}}{35} f_4(0)Z_{40}(\Theta,\Phi)$$
$$+2\left(\frac{\pi}{15}\right)^{1/2} f_2\left(\frac{4}{5}\right)Z_{22}^{(c)}(\Theta,\Phi)$$
$$+\frac{2}{21}\left(\frac{\pi}{5}\right)^{1/2} f_2\left(\frac{28}{5}\right)Z_{20}(\Theta,\Phi) - \frac{4\pi^{1/2}}{15} f_0(2)Z_{00}(\Theta,\Phi),$$

$$\langle y|T_{yy}|y\rangle = 2\left(\frac{\pi}{35}\right)^{1/2} f_4(0)Z_{44}^{(c)}(\Theta,\Phi) + \frac{4}{7}\left(\frac{\pi}{5}\right)^{1/2} f_4(0)Z_{42}^{(c)}(\Theta,\Phi) + \frac{6\pi^{1/2}}{35}$$
$$\times f_4(0)Z_{40}(\Theta,\Phi) - \frac{22}{7}\left(\frac{\pi}{15}\right)^{1/2} f_2\left(\frac{56}{55}\right)Z_{22}^{(c)}(\Theta,\Phi) - \frac{22}{21}\left(\frac{\pi}{5}\right)^{1/2} f_2\left(\frac{56}{55}\right)$$
$$\times Z_{20}(\Theta,\Phi) + \frac{8\pi^{1/2}}{15} f_0(2)Z_{00}(\Theta,\Phi),$$

$$\langle y|T_{zz}|y\rangle = -\frac{4}{7}\left(\frac{\pi}{5}\right)^{1/2} f_4(0)Z_{42}^{(c)}(\Theta,\Phi) - \frac{8\pi^{1/2}}{35} f_4(0)Z_{40}(\Theta,\Phi) + \frac{8}{7}\left(\frac{\pi}{15}\right)^{1/2}$$
$$\times f_2\left(\frac{7}{5}\right)Z_{22}^{(c)}(\Theta,\Phi) + \frac{20}{21}\left(\frac{\pi}{5}\right)^{1/2} f_2\left(\frac{14}{25}\right)Z_{20}(\Theta,\Phi) - \frac{4\pi^{1/2}}{15} f_0(2)Z_{00}(\Theta,\Phi),$$

$$\langle y|T_{xy}|y\rangle = -2\left(\frac{\pi}{35}\right)^{1/2} f_4(0)Z_{44}^{(s)}(\Theta,\Phi) - \frac{2}{7}\left(\frac{\pi}{5}\right)^{1/2} f_4(0)Z_{42}^{(s)}(\Theta,\Phi) + \frac{18}{7}\left(\frac{\pi}{15}\right)^{1/2}$$
$$\times f_2\left(\frac{14}{15}\right)Z_{22}^{(s)}(\Theta,\Phi),$$

$$\langle y|T_{yz}|y\rangle = -\left(\frac{2\pi}{35}\right)^{1/2} f_4(0)Z_{43}^{(s)}(\Theta,\Phi) - \frac{3}{7}\left(\frac{2\pi}{5}\right)^{1/2} f_4(0)Z_{41}^{(s)}(\Theta,\Phi)$$
$$+\frac{18}{7}\left(\frac{\pi}{15}\right)^{1/2} f_2\left(\frac{14}{15}\right)Z_{21}^{(s)}(\Theta,\Phi),$$

$$\langle y|T_{zx}|y\rangle = -\left(\frac{2\pi}{35}\right)^{1/2} f_4(0)Z_{43}^{(c)}(\Theta,\Phi) - \frac{1}{7}\left(\frac{2\pi}{5}\right)^{1/2} f_4(0)Z_{41}^{(c)}(\Theta,\Phi)$$
$$+\frac{6}{7}\left(\frac{\pi}{15}\right)^{1/2} f_2(0)Z_{21}^{(c)}(\Theta,\Phi),$$

$$\langle z|T_{xx}|z\rangle = \frac{4}{7}\left(\frac{\pi}{5}\right)^{1/2} f_4(0)Z_{42}^{(c)}(\Theta,\Phi) - \frac{8\pi^{1/2}}{35} f_4(0)Z_{40}(\Theta,\Phi)$$
$$+\frac{6}{7}\left(\frac{\pi}{15}\right)^{1/2} f_2(0)Z_{22}^{(c)}(\Theta,\Phi)$$
$$-\frac{22}{21}\left(\frac{\pi}{5}\right)^{1/2} f_2\left(\frac{56}{55}\right)Z_{20}(\Theta,\Phi) - \frac{4\pi^{1/2}}{15} f_0(2)Z_{00}(\Theta,\Phi),$$

$$\langle z|T_{yy}|z\rangle = -\frac{4}{7}\left(\frac{\pi}{5}\right)^{1/2} f_4(0)Z_{42}^{(c)}(\Theta,\Phi) - \frac{8\pi^{1/2}}{35} f_4(0)Z_{40}(\Theta,\Phi)$$
$$-\frac{6}{7}\left(\frac{\pi}{15}\right)^{1/2} f_2(0)Z_{22}^{(c)}(\Theta,\Phi) - \frac{22}{21}\left(\frac{\pi}{5}\right)^{1/2} f_2\left(\frac{56}{55}\right)Z_{20}(\Theta,\Phi)$$
$$-\frac{4\pi^{1/2}}{15} f_0(2)Z_{00}(\Theta,\Phi),$$

$$\langle z|T_{zz}|z\rangle = \frac{16\pi^{1/2}}{35} f_4(0)Z_{40}(\Theta,\Phi) + \frac{44}{21}\left(\frac{\pi}{5}\right)^{1/2} f_2\left(\frac{56}{55}\right)Z_{20}(\Theta,\Phi)$$
$$+\frac{8\pi^{1/2}}{15} f_0(2)Z_{00}(\Theta,\Phi),$$

$$\langle z|T_{xy}|z\rangle = \frac{4}{7}\left(\frac{\pi}{5}\right)^{1/2} f_4(0)Z_{42}^{(s)}(\Theta,\Phi) + \frac{6}{7}\left(\frac{\pi}{15}\right)^{1/2} f_2(0)Z_{22}^{(s)}(\Theta,\Phi),$$

$$\langle z|T_{yz}|z\rangle = \frac{4}{7}\left(\frac{2\pi}{5}\right)^{1/2} f_4(0) Z_{41}^{(s)}(\Theta, \Phi) + \frac{18}{7}\left(\frac{\pi}{15}\right)^{1/2} f_2\left(\frac{14}{15}\right) Z_{21}^{(s)}(\Theta, \Phi),$$

$$\langle z|T_{zx}|z\rangle = \frac{4}{7}\left(\frac{2\pi}{5}\right)^{1/2} f_4(0) Z_{41}^{(c)}(\Theta, \Phi) + \frac{18}{7}\left(\frac{\pi}{15}\right)^{1/2} f_2\left(\frac{14}{15}\right) Z_{21}^{(c)}(\Theta, \Phi),$$

$$\langle y|T_{xx}|x\rangle = 2\left(\frac{\pi}{35}\right)^{1/2} f_4(0) Z_{44}^{(s)}(\Theta, \Phi) - \frac{2}{7}\left(\frac{\pi}{5}\right)^{1/2} f_4(0) Z_{42}^{(s)}(\Theta, \Phi) + \frac{4}{7}\left(\frac{\pi}{15}\right)^{1/2} f_2\left(\frac{7}{5}\right) Z_{22}^{(s)}(\Theta, \Phi),$$

$$\langle y|T_{yy}|x\rangle = -2\left(\frac{\pi}{35}\right)^{1/2} f_4(0) Z_{44}^{(s)}(\Theta, \Phi) - \frac{2}{7}\left(\frac{\pi}{5}\right)^{1/2} f_4(0) Z_{42}^{(s)}(\Theta, \Phi) + \frac{4}{7}\left(\frac{\pi}{15}\right)^{1/2} f_2\left(\frac{7}{5}\right) Z_{22}^{(s)}(\Theta, \Phi),$$

$$\langle y|T_{zz}|x\rangle = \frac{4}{7}\left(\frac{\pi}{5}\right)^{1/2} f_4(0) Z_{42}^{(s)}(\Theta, \Phi) - \frac{8}{7}\left(\frac{\pi}{15}\right)^{1/2} f_2\left(\frac{7}{5}\right) Z_{22}^{(s)}(\Theta, \Phi),$$

$$\langle y|T_{xy}|x\rangle = -2\left(\frac{\pi}{35}\right)^{1/2} f_4(0) Z_{44}^{(c)}(\Theta, \Phi) + \frac{2\pi^{1/2}}{35} f_4(0) Z_{40}(\Theta, \Phi) - \frac{4}{7}\left(\frac{\pi}{5}\right)^{1/2} f_2\left(\frac{7}{5}\right) Z_{20}(\Theta, \Phi) + \frac{2\pi^{1/2}}{5} f_0(2) Z_{00}(\Theta, \Phi),$$

$$\langle y|T_{yz}|x\rangle = -\left(\frac{2\pi}{35}\right)^{1/2} f_4(0) Z_{43}^{(c)}(\Theta, \Phi) - \frac{1}{7}\left(\frac{2\pi}{5}\right)^{1/2} f_4(0) Z_{41}^{(c)}(\Theta, \Phi) + \frac{6}{7}\left(\frac{\pi}{15}\right)^{1/2} f_2\left(\frac{7}{5}\right) Z_{21}^{(c)}(\Theta, \Phi),$$

$$\langle y|T_{zx}|x\rangle = \left(\frac{2\pi}{35}\right)^{1/2} f_4(0) Z_{43}^{(s)}(\Theta, \Phi) - \frac{1}{7}\left(\frac{2\pi}{5}\right)^{1/2} f_4(0) Z_{41}^{(s)}(\Theta, \Phi) + \frac{6}{7}\left(\frac{\pi}{15}\right)^{1/2} f_2\left(\frac{7}{5}\right) Z_{21}^{(s)}(\Theta, \Phi),$$

$$\langle z|T_{xx}|y\rangle = \left(\frac{2\pi}{35}\right)^{1/2} f_4(0) Z_{43}^{(s)}(\Theta, \Phi) - \frac{1}{7}\left(\frac{2\pi}{5}\right)^{1/2} f_4(0) Z_{41}^{(s)}(\Theta, \Phi) - \frac{8}{7}\left(\frac{\pi}{15}\right)^{1/2} f_2\left(\frac{7}{5}\right) Z_{21}^{(s)}(\Theta, \Phi),$$

$$\langle z|T_{yy}|y\rangle = -\left(\frac{2\pi}{35}\right)^{1/2} f_4(0) Z_{43}^{(s)}(\Theta, \Phi) - \frac{3}{7}\left(\frac{2\pi}{5}\right)^{1/2} f_4(0) Z_{41}^{(s)}(\Theta, \Phi) + \frac{4}{7}\left(\frac{\pi}{15}\right)^{1/2} f_2\left(\frac{7}{5}\right) Z_{21}^{(s)}(\Theta, \Phi),$$

$$\langle z|T_{zz}|y\rangle=\frac{4}{7}\left(\frac{2\pi}{5}\right)^{1/2}f_4(0)Z_{41}^{(s)}(\Theta,\Phi)+\frac{4}{7}\left(\frac{\pi}{15}\right)^{1/2}f_2\left(\frac{7}{5}\right)Z_{21}^{(s)}(\Theta,\Phi),$$

$$\langle z|T_{xy}|y\rangle=-\left(\frac{2\pi}{35}\right)^{1/2}f_4(0)Z_{43}^{(c)}(\Theta,\Phi)-\frac{1}{7}\left(\frac{2\pi}{5}\right)^{1/2}f_4(0)Z_{41}^{(c)}(\Theta,\Phi)$$
$$+\frac{6}{7}\left(\frac{\pi}{15}\right)^{1/2}f_2\left(\frac{7}{5}\right)Z_{21}^{(c)}(\Theta,\Phi),$$

$$\langle z|T_{yz}|y\rangle=-\frac{4}{7}\left(\frac{\pi}{5}\right)^{1/2}f_4(0)Z_{42}^{(c)}(\Theta,\Phi)-\frac{8\pi^{1/2}}{35}f_4(0)Z_{40}(\Theta,\Phi)$$
$$-\frac{6}{7}\left(\frac{\pi}{15}\right)^{1/2}f_2\left(\frac{7}{5}\right)Z_{22}^{(c)}(\Theta,\Phi)+\frac{2}{7}\left(\frac{\pi}{5}\right)^{1/2}f_2\left(\frac{7}{5}\right)Z_{20}(\Theta,\Phi)$$
$$+\frac{2\pi^{1/2}}{5}f_0(2)Z_{00}(\Theta,\Phi),$$

$$\langle z|T_{zx}|y\rangle=\frac{4}{7}\left(\frac{\pi}{5}\right)^{1/2}f_4(0)Z_{42}^{(s)}(\Theta,\Phi)+\frac{6}{7}\left(\frac{\pi}{15}\right)^{1/2}f_2\left(\frac{7}{5}\right)Z_{22}^{(s)}(\Theta,\Phi),$$

$$\langle x|T_{xx}|z\rangle=\left(\frac{2\pi}{35}\right)^{1/2}f_4(0)Z_{43}^{(c)}(\Theta,\Phi)-\frac{3}{7}\left(\frac{2\pi}{5}\right)^{1/2}f_4(0)Z_{41}^{(c)}(\Theta,\Phi)$$
$$+\frac{4}{7}\left(\frac{\pi}{15}\right)^{1/2}f_2\left(\frac{7}{5}\right)Z_{21}^{(c)}(\Theta,\Phi),$$

$$\langle x|T_{yy}|z\rangle=-\left(\frac{2\pi}{35}\right)^{1/2}f_4(0)Z_{43}^{(c)}(\Theta,\Phi)-\frac{1}{7}\left(\frac{2\pi}{5}\right)^{1/2}f_4(0)Z_{41}^{(c)}(\Theta,\Phi)$$
$$-\frac{8}{7}\left(\frac{\pi}{15}\right)^{1/2}f_2\left(\frac{7}{5}\right)Z_{21}^{(c)}(\Theta,\Phi),$$

$$\langle x|T_{zz}|z\rangle=\frac{4}{7}\left(\frac{2\pi}{5}\right)^{1/2}f_4(0)Z_{41}^{(c)}(\Theta,\Phi)+\frac{4}{7}\left(\frac{\pi}{15}\right)^{1/2}f_2\left(\frac{7}{5}\right)Z_{21}^{(c)}(\Theta,\Phi),$$

$$\langle x|T_{xy}|z\rangle=\left(\frac{2\pi}{35}\right)^{1/2}f_4(0)Z_{43}^{(s)}(\Theta,\Phi)-\frac{1}{7}\left(\frac{2\pi}{5}\right)^{1/2}f_4(0)Z_{41}^{(s)}(\Theta,\Phi)$$
$$+\frac{6}{7}\left(\frac{\pi}{15}\right)^{1/2}f_2\left(\frac{7}{5}\right)Z_{21}^{(s)}(\Theta,\Phi),$$

$$\langle x|T_{yz}|z\rangle=\frac{4}{7}\left(\frac{\pi}{5}\right)^{1/2}f_4(0)Z_{42}^{(s)}(\Theta,\Phi)+\frac{6}{7}\left(\frac{\pi}{15}\right)^{1/2}f_2\left(\frac{7}{5}\right)Z_{22}^{(s)}(\Theta,\Phi),$$

$$\langle x|T_{zx}|z\rangle=\frac{4}{7}\left(\frac{\pi}{5}\right)^{1/2}f_4(0)Z_{42}^{(c)}(\Theta,\Phi)-\frac{8\pi^{1/2}}{35}f_4(0)Z_{40}(\Theta,\Phi)$$
$$+\frac{6}{7}\left(\frac{\pi}{15}\right)^{1/2}f_2\left(\frac{7}{5}\right)Z_{22}^{(c)}(\Theta,\Phi)$$
$$+\frac{2}{7}\left(\frac{\pi}{5}\right)^{1/2}f_2\left(\frac{7}{5}\right)Z_{20}(\Theta,\Phi)+\frac{2\pi^{1/2}}{5}f_0(2)Z_{00}(\Theta,\Phi).$$

(c) The Integrals $\langle \Psi_i | l_{N\alpha}/r_N^3 | \Psi_j \rangle$

The integrals $\langle \Psi_i | l_{N\alpha}/r_N^3 | \Psi_j \rangle$ are given by

$$i\langle x|l_{Nx}/r_N^3|y\rangle = -\left(\frac{\pi}{15}\right)^{1/2}(V_1+W_2)Z_{21}^{(c)}(\Theta,\Phi),$$

$$i\langle x|l_{Ny}/r_N^3|y\rangle = -\left(\frac{\pi}{15}\right)^{1/2}(V_1+W_2)Z_{21}^{(s)}(\Theta,\Phi),$$

$$i\langle x|l_{Nz}/r_N^3|y\rangle = -\frac{2}{3}\left(\frac{\pi}{5}\right)^{1/2}(V_1+W_2)Z_{20}(\Theta,\Phi)+\frac{2\pi^{1/2}}{3}(V_1+W_0)Z_{00}(\Theta,\Phi),$$

$$i\langle y|l_{Nx}/r_N^3|z\rangle = -\left(\frac{\pi}{15}\right)^{1/2}(V_1+W_2)Z_{22}^{(c)}(\Theta,\Phi)+\frac{1}{3}\left(\frac{\pi}{5}\right)^{1/2}(V_1+W_2)Z_{20}(\Theta,\Phi)$$
$$+\frac{2\pi^{1/2}}{3}(V_1+W_0)Z_{00}(\Theta,\Phi),$$

$$i\langle y|l_{Ny}/r_N^3|z\rangle = -\left(\frac{\pi}{15}\right)^{1/2}(V_1+W_2)Z_{22}^{(s)}(\Theta,\Phi),$$

$$i\langle y|l_{Nz}/r_N^3|z\rangle = -\left(\frac{\pi}{15}\right)^{1/2}(V_1+W_2)Z_{21}^{(c)}(\Theta,\Phi),$$

$$i\langle z|l_{Nx}/r_N^3|x\rangle = -\left(\frac{\pi}{15}\right)^{1/2}(V_1+W_2)Z_{22}^{(s)}(\Theta,\Phi),$$

$$i\langle z|l_{Ny}/r_N^3|x\rangle = \left(\frac{\pi}{15}\right)^{1/2}(V_1+W_2)Z_{22}^{(c)}(\Theta,\Phi)+\frac{1}{3}\left(\frac{\pi}{5}\right)^{1/2}(V_1+W_2)Z_{20}(\Theta,\Phi)$$
$$+\frac{2\pi^{1/2}}{3}(V_1+W_0)Z_{00}(\Theta,\Phi),$$

$$i\langle z|l_{Nz}/r_N^3|x\rangle = -\left(\frac{\pi}{15}\right)^{1/2}(V_1+W_2)Z_{21}^{(s)}(\Theta,\Phi).$$

REFERENCES

1. R. J. KURLAND AND B. R. MCGARVEY, *J. Magn. Reson.* **2,** 286 (1970).
2. A. D. BUCKINGHAM AND P. J. STILES, *Mol. Phys.* **24,** 99 (1972).
3. P. J. STILES, *Mol. Phys.* **27,** 501 (1974).
4. P. J. STILES, *Mol. Phys.* **29,** 1271 (1975).
5. J. P. RILEY AND W. T. RAYNES, *Mol. Phys.* **33,** 619 (1977).
6. R. M. GOLDING, R. O. PASCUAL, AND J. VRBANCICH, *Mol. Phys.* **31,** 731 (1976).
7. R. M. GOLDING, *Pure Appl. Chem.* **32,** 123 (1972), and references therein.
8. W. B. LEWIS, J. A. JACKSON, J. F. LEMONS, AND H. TAUBE, *J. Chem. Phys.* **36,** 694 (1962).
9. R. M. GOLDING AND M. P. HALTON, *Aust. J. Chem.* **25,** 2577 (1972).
10. B. BLEANEY, C. M. DOBSON, B. A. LEVINE, R. B. MARTIN, R. J. P. WILLIAMS, AND A. V. XAVIER, *J. Chem. Soc. Chem. Commun.* 791 (1972).
11. M. KAINOSHR, K. AJISAKA, AND K. TORI, *Chem. Lett.* 1061 (1972).
12. H. A. BERGEN AND R. M. GOLDING, *Aust. J. Chem.* **30,** 2361 (1977).

13. R. M. GOLDING, R. O. PASCUAL, AND L. C. STUBBS, *Mol. Phys.* **31,** 1933 (1976).
14. R. M. GOLDING AND L. C. STUBBS, *Proc. Roy. Soc., Ser. A.* **354,** 223 (1977).
15. R. M. GOLDING, "Applied Wave Mechanics," Van Nostrand, London, 1969.
16. R. M. GOLDING AND L. C. STUBBS, *Proc. Roy. Soc., Ser. A.*, **362,** 525 (1978).
17. R. M. GOLDING, *Mol. Phys.* **8,** 561 (1964).
18. J. S. GRIFFITH, "The Theory of Transition-Metal Ions," Cambridge Univ. Press, London/New York, 1961.